POTENTIAL AND LIMITATIONS OF FORWARD-LOOKING BISTATIC SAR

Ingo Walterscheid, Thomas Espeter, Jens Klare, Andreas R. Brenner, Joachim H. G. Ender

Fraunhofer Institute for High Frequency Physics and Radar Techniques FHR,
Neuenahrer Str. 20, 53343 Wachtberg, Germany
Email: ingo.walterscheid@fhr.fraunhofer.de

1. INTRODUCTION

Bistatic synthetic aperture radar (SAR) operates with spatially separated transmit and receive antennas that are mounted on separated platforms. Such a configuration enables a variety of data acquisition geometries to achieve benefits like the increased information content of bistatic SAR data. A bistatic imaging radar, which uses a special acquisition geometry, where the receive antenna looks in forward direction, is called bistatic forward-looking SAR. In contrast to common monostatic SAR systems, it is possible to get high resolution images in forward direction, which is highly desirebale for many applications, e. g., flight safety during landing approach.

Common monostatic SAR systems with transmitter and receiver on one platform are not useful to image in forward direction due to left/right ambiguities and poor Doppler resolution. Nevertheless, in the past, several techniques have been proposed to improve the azimuth resolution and to reduce the left/right ambiguities of a monostatic forward-looking SAR. One of the first approaches was based on Doppler-Beam-Sharpening SAR (DBS) using a rotating reflector antenna [1]. To enhance the azimuth resolution DBS was extended by using specific illumination functions [2]. Another approach with one transmitting and two or multiple receiving antennas perpendicular to the flight direction is discussed in [3]. A forward-looking SAR demonstrator (SIREV) using a linear array antenna perpendicular to the flight direction was realized and described in [4]. Although these techniques are more or less useful for forward-looking SAR, the Doppler resolution is still a multiple of the Doppler resolution obtained by a side-looking SAR. Furthermore, these techniques increase the system complexity significantly which limits their applicability only to large airborne platforms. In recent years, some theoretical investigations on bistatic forward-looking SAR have been published, e. g. [5].

This paper presents an overview of forward-looking bistatic SAR and analyzes the imaging capability of a moving forward-looking receiver in a bistatic scenario with respect to spatial resolution and the orientation of the iso-range and iso-Doppler contours. Furthermore, the results of a bistatic SAR experiment with the radar satellite TerraSAR-X as transmitter and the airborne SAR system PAMIR as receiver are presented to demonstrate for the first time imaging in forward- or backward-looking direction. For convenience, the receiving antenna was mounted on the aircraft's loading ramp and looked backwards. Due to identical image properties and the same challenges for forward- and backward-looking sensors, this experiment also demonstrates the feasibility of forward-looking bistatic SAR.

2. APPLICATIONS

Radar imaging in forward direction becomes more and more attractive for a variety of applications. The most popular one is to provide images of the earth ground for aircraft's landing assistance. This could improve the landing safety, especially in poor visibility conditions and in situations where external electronic guidance systems are unavailable or the imaging of the runway is desired. Assumed that the scene is illuminated by an appropriate transmitter, a cost-effective receive-only system mounted on an aircraft could help the pilot by the identification of obstacles in flight direction (collision warning system), observation, navigation and approaches independent of weather conditions and time of day or night. Such a receiver needs no complex antenna technology, it could be very compact, lightweight and low-cost. Especially, systems for small aircrafts or unmanned aerial vehicles (UAV) would benefit from these features.

3. ISO-RANGE AND ISO-DOPPLER CONTOURS

3.1. Definitions

The imaging quality of a scene for a given bistatic geometry can be evaluated by plotting the iso-range and iso-Doppler contours in one diagram (imaging grid). The density and the orientation of the contours determine the image quality. The higher the contour density, the better the appropriate resolution. Furthermore, to get the best target resolution in two dimensions, the angle between the iso-range and iso-Doppler lines should be $90°$. In the worst case the angle is zero degree, which means that we get a target resolution only in one dimension.

The sets of all points with a fixed range $\tilde{R}$, or a fixed Doppler frequency $\tilde{F}$ are given by [6]

$$M_R(T; \tilde{R}) = \left\{ \vec{r} : R(T; \vec{r}) = \tilde{R} \right\},$$
$$M_F(T; \tilde{F}) = \left\{ \vec{r} : -\frac{1}{\lambda} \frac{\partial}{\partial T} R(T, \vec{r}) = \tilde{F} \right\} \tag{1}$$

and their intersections with the (x, y)-plane by $\mathcal{M}_R(T; \tilde{R})$ and $\mathcal{M}_F(T; \tilde{F})$. The bistatic range $R(T; \vec{r})$ is given by the sum of transmitter-to-target range $R_1(T; \vec{r})$ and receiver-to-target range $R_2(T; \vec{r})$

$$R(T; \vec{r}) = R_1(T; \vec{r}) + R_2(T; \vec{r}), \tag{2}$$

with T the slow time variable. The derivative of the bistatic range is given by the sum of $\partial R_1(T, \vec{r})/\partial T$ and $\partial R_2(T, \vec{r})/\partial T$, which are the projections of the transmitting and receiving velocity vectors onto their respective target line-of-sights.

As generally known, the points of $M_R(T; \tilde{R})$ lie on the surface of an ellipsoid with the transmitter and receiver in its focal points and $\mathcal{M}_R(T; \tilde{R})$ will be ellipses as intersections of an ellipsoid with a plane (Iso-range lines). The intersections of $M_F(T; \tilde{F})$ with a plane are called the iso-Doppler lines.

3.2. Imaging grid of a forward-looking sensor

High resolution imaging in flight direction is not possible using a common monostatic SAR system due to the following reasons. First, ground targets situated symmetrically about the flight pass have the same Doppler history and cause ambiguities in the SAR image (left/right ambiguities). Second, the gradient of the Doppler frequency is very small in flight direction in comparison to the boresight side-looking direction, which results in a poor Doppler resolution. Third, in forward-looking direction the angle between the direction of Doppler and range resolution is very small and in the worst case zero, resulting in no resolution in one dimension. These characteristics are presented in Fig. 1a. It shows the iso-range (red) and iso-Doppler (blue) lines of a monostatic SAR. The position and heading of the sensor is characterized by the arrow and the typical illuminated areas for a side-looking (solid line) and forward-looking (dashed line) sensor are plotted. The different forms of the resolution cells in the forward and sideward illuminated areas are clearly visible.

Fig. 1b shows the iso-range and iso-Doppler lines on ground for a bistatic constellation, where the antenna of the transmitter (big arrow) is side-looking and the antenna of the receiver (small arrow) is forward-looking. Both platforms move in the same direction as indicated by the arrows. Now, in most part of the common illuminated area the resolution cells are small and the angle between the gradient of iso-range and iso-Doppler is satisfying, except at the outermost left side of the illuminated area, where resolution only in one dimension is available.

4. BACKWARD-LOOKING SAR EXPERIMENT WITH TERRASAR-X AND PAMIR

4.1. Geometry

After several successful experiments using TerraSAR-X as illuminator and PAMIR as receiver [7, 8] the first non-side-looking SAR experiment using both systems was carried out in November 2009. The X-band SAR-satellite TerraSAR-X operated in the high-resolution spotlight mode, which resulted in an illumination time of the scene for about 3 seconds. The bandwidth was 300 MHz at a center frequency of 9.65 GHz. The geometry and parameters of the experiment are presented in Fig. 2.

The airborne SAR/GMTI system PAMIR (Phased Array Multifunctional Imaging Radar), developed at the Fraunhofer Institute for High Frequency Physics and Radar Techniques (FHR), was employed as the passive receiver onboard a Transall C-160 aircraft. Due to the fact that the imaging conditions in forward or backward-looking direction are the same and the possibility to install a backward-looking antenna on the aircraft's loading ramp, we chose a backward-looking geometry to
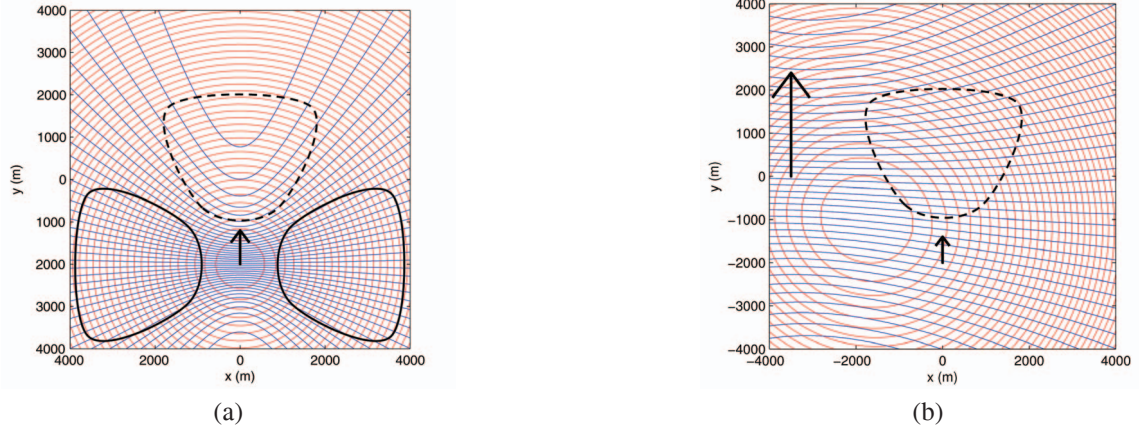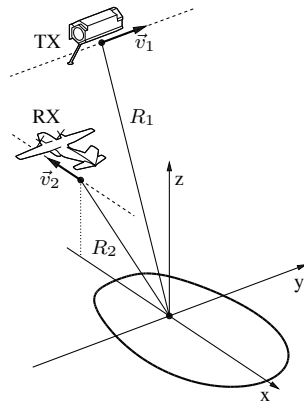
(a)   (b)

Fig. 1. (a) Iso-range (red) and iso-Doppler (blue) contours of a monostatic SAR (arrow) and footprints for a side-looking (solid line) and forward-looking (dashed line) antenna. (b) Corresponding contours for a bistatic SAR constellation with a forward-looking receiver (small arrow) and a side-looking transmitter (big arrow).

	PAMIR	TerraSAR-X
Slant range	2.9 km	559 km
Altitude	1.5 km	515 km
Incidence angle	60°	24°
Azimuth beamwidth	27°	0.33°
Elevation beamwidth	27°	2.3°
Platform velocity	100 m/s	7 600 m/s
PRF	1 490 Hz	4 471 Hz
Wavelength	3.1 cm	
Signal bandwidth	300 MHz	
Polarization	VV	
Acquisition time	3 s	

Fig. 2. Geometry and parameters of the spaceborne/airborne SAR experiment.

demonstrate the feasibility of SAR imaging in flight direction. Using a standard gain horn and low-noise amplifiers instead of PAMIR's antenna frontend led to an increased beamwidth of 27° in azimuth and elevation, respectively.

An additional antenna was mounted on top of the aircraft's fuselage to receive the direct satellite signal for synchronization and reference purposes. This signal was used by the pulse synchronization system, which triggered PAMIR's timing controller. After activation, the timing controller worked with a fixed PRF, which in this case was about one third of the transmitter's PRF. A small PRF offset remained due to the systems' different reference clocks. This induced a linear range-walk of the recorded signal, which was removed during the data processing.

4.2. Processing and experimental results

A theoretical analysis of the experiment shows, that the ground range resolution is about 0.7 m and the Doppler resolution varies between 1.2 m at the top and 3 m at the bottom of the image. The calculated iso-range and iso-Doppler contours for the experiment are shown in Fig. 3.

The well focused bistatic SAR image acquired in backward-looking direction is presented in Fig. 4. The scene size is about 5 km x 3 km. It was processed using a bistatic backprojection processor and shows a part of the village Manching, Bavaria, Germany on the left side and a part of an airfield on the right side. The reason for the ambiguities and poor Doppler resolution in the lower left corner can be explained by analyzing the appropriate imaging grid in Fig. 3. In this area the range and Doppler contours are nearly parallel resulting in a poor cross-track resolution. Nevertheless, the center of the image especially the runway for flight assistance applications is clearly visible.
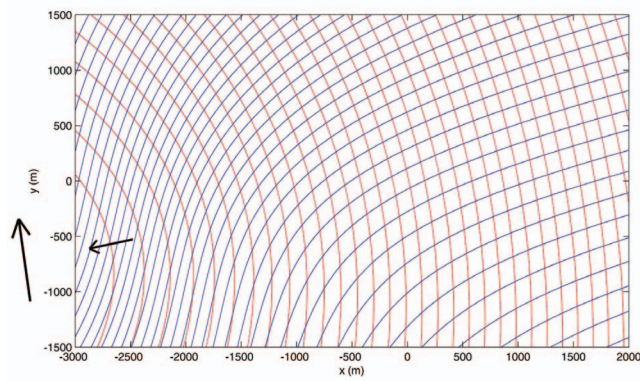
Fig. 3. Iso-range and iso-Doppler contours of the backward-looking experiment. The small arrow symbolizes the position and flight direction of the backward-looking receiver and the big arrow symbolizes the flight direction of TerraSAR-X.
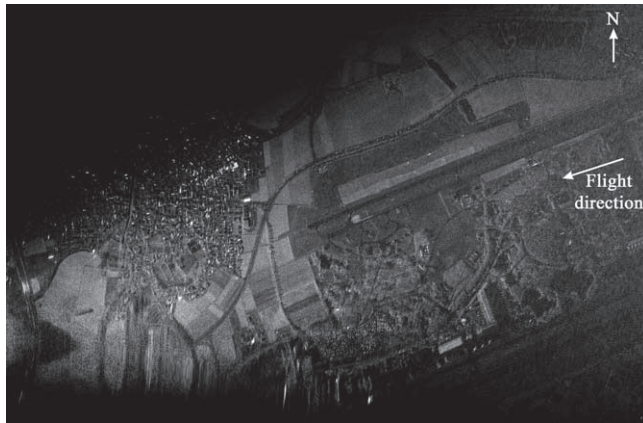

Fig. 4. Bistatic SAR image in backward-looking direction.

5. REFERENCES

[1] D. R. Wehner, *High-Resolution Radar*, Artech House, 1995.

[2] A. K. Löhner, "Improved azimuthal resolution of forward looking SAR by sophisticated antenna illumination function design," *Proc. Inst. Elect Eng.–Radar Sonar Navig.*, vol. 145, no. 2, pp. 128–134, Apr. 1998.

[3] Shengli Dai, Min Liu, Yajun Sun, and W. Wiesbeck, "The latest development of high resolution imaging for forward looking SAR with multiple receiving antennas," in *Proc. IEEE IGARSS*, July 2001, vol. 3, pp. 1433–1435.

[4] G. Krieger, J. Mittermayer, M. Wendler, F. Witte, and A. Moreira, "SIREV-sector imaging radar for enhanced vision," in *Proc. Int. Symp. on Image and Signal Processing and Analysis ISPA 2001*, Pula, Croatia, June 19–21, 2001, pp. 377–382.

[5] Xiaolan Qiu, Donghui Hu, and Chibiao Ding, "Some reflections on bistatic SAR of forward-looking configuration," *IEEE Geosci. Remote Sens. Lett.*, vol. 5, no. 4, pp. 735–739, Oct. 2008.

[6] J. Ender, "Signal theoretical aspects of bistatic SAR," in *Proc. IEEE IGARSS*, Toulouse, France, July 2003, pp. 1438–1441.

[7] I. Walterscheid, T. Espeter, C. Gierull, J. Klare, A. Brenner, and J. Ender, "Results and analysis of hybrid bistatic SAR experiments with spaceborne, airborne and stationary sensors," in *Proc. IEEE IGARSS*, Cape Town, South Africa, July 2009, vol. 2, pp. 238–241.

[8] I. Walterscheid, T. Espeter, A. Brenner, J. Klare, J. Ender, H. Nies, R. Wang, and O. Loffeld, "Bistatic SAR experiments with PAMIR and TerraSAR-X - setup, processing, and image results," *IEEE Trans. Geosci. Remote Sens.*, accepted.